Submitted to Nuclear Instruments and Methods

UCRL-18822
Preprint

cy. 2

RECEIVED
LAWRENCE
RADIATION LABORATORY
APR 25 1969
LIBRARY AND
DOCUMENTS SECTION

SLIT SCATTERING EFFECTS WITH MEDIUM ENERGY ALPHA PARTICLES AND PROTONS

F. G. Resmini, A. D. Bacher, D. J. Clark, E. A. McClatchie, and R. De Swiniarski

April 1969

AEC Contract No. W-7405-eng-48

TWO-WEEK LOAN COPY

This is a Library Circulating Copy which may be borrowed for two weeks. For a personal retention copy, call Tech. Info. Division, Ext. 5545

UCRL-18822
cy. 2

LAWRENCE RADIATION LABORATORY
UNIVERSITY of CALIFORNIA BERKELEY

DISCLAIMER

This document was prepared as an account of work sponsored by the United States Government. While this document is believed to contain correct information, neither the United States Government nor any agency thereof, nor the Regents of the University of California, nor any of their employees, makes any warranty, express or implied, or assumes any legal responsibility for the accuracy, completeness, or usefulness of any information, apparatus, product, or process disclosed, or represents that its use would not infringe privately owned rights. Reference herein to any specific commercial product, process, or service by its trade name, trademark, manufacturer, or otherwise, does not necessarily constitute or imply its endorsement, recommendation, or favoring by the United States Government or any agency thereof, or the Regents of the University of California. The views and opinions of authors expressed herein do not necessarily state or reflect those of the United States Government or any agency thereof or the Regents of the University of California.

SLIT SCATTERING EFFECTS WITH MEDIUM ENERGY ALPHA PARTICLES AND PROTONS*

F. G. Resmini,† A. D. Bacher, D. J. Clark, E. A. McClatchie, and R. De Swiniarski††

Lawrence Radiation Laboratory
University of California
Berkeley, California 94720

April 1969

ABSTRACT

The slit scattering effect has been measured for medium energy protons and alpha particles on aluminum, brass and tantalum slits. A successful comparison with the theoretical treatment of Courant has enabled us to predict the slit scattering effect for our experimental conditions lending credence to the application of the Courant theory to other experimental conditions.

*Work performed under the auspices of the U.S. Atomic Energy Commission.

†On leave from the University of Milano, Milan, Italy.

††NATO-Fulbright Fellow: permanent address: Institut des Sciences Nucleaires, Grenoble, France.

1. Introduction

The continuum background arising from particles scattered by slits in front of detectors is of importance in high resolution nuclear spectroscopy experiments and may set a lower limit on the observable cross sections. The purpose of the present experiment was to measure the scattering arising from slits of different materials, profiles and surface finishes. This study was prompted by the lack of such measurements in the literature, although some work in this direction has been reported[1]). Our experimental conditions were chosen to allow an easy comparison with the existing theoretical treatments[2,3]). For this reason we are concerned only with slits placed immediately in front of a counter, in which particles scattered at all angles are detected. No attempt has been made to measure the angular distribution of the particles, which might be more relevant in other applications, e.g. defining slits in beam transport lines.

2. Experimental Method

Fig. 1 sketches the experimental conditions. Beams from the Berkeley 88-inch cyclotron were energy analyzed to 0.02% FWHM and focused at the center of the scattering chamber, where a cooled Si(Li) counter, 12 mm in diameter, was placed. Various slits, of 2 mm width and 10 mm height, could then be positioned successively in front of the detector at a distance of about 1 mm from it. For each run the counters were carefully selected for high resolution ($\leqslant$ 10 keV, FWHM for 1 MeV electrons). The condition of the counter was periodically checked by taking runs without slits. The detector was replaced whenever radiation damage effects became apparent (typically after a total exposure of $\approx 10^8$ particles).

The beam was focused to a spot 6 mm wide by 1 mm high, i.e. considerably smaller than the counter dimensions. For our radial emittance of 10 mm-mrad this implies a beam with radial divergence less than 1 mrad. The uniformity of illumination of the slits was checked by sweeping the beam by ± 1 mm across a 0.12 mm slit and measuring the transmitted intensity. This was found to remain constant to within ± 10%. All measurements were taken with a beam intensity of 1000-1500 particles per second, with 20 MeV protons and with alpha particles of 50 and 80 MeV.

Some of the slit profiles used are shown at the bottom of fig. 1. The materials used were brass, aluminum, and tantalum. According to previous calculations[3]) brass and tantalum are two of the materials which minimize the slit scattering effect. The surfaces were hand-polished so that surface scratches were typically less than 1-2 microns in depth. For the purpose of comparison straight-edged slits with machine-cut surfaces were also used. The surface irregularities in this case were up to 20 microns deep. The thickness of all slits was the stopping thickness for the particles plus 15%, to allow a margin for straggling.

3. Experimental Results

Figs. 2 and 3 provide examples of typical experimental data. Fig. 2 presents spectra obtained with 20 MeV protons: without slits at the top of the figure and with polished, straight-edged, brass slits at the bottom. The energy range covered by these spectra includes about 2 MeV below the main peak. The effect of slit scattering is quite evident. Fig. 3 presents the spectra obtained over the entire range of 20 MeV. Some excited states of

^{28}Si, indicated for reference, are partially masked by the background arising from the slits. In this spectrum the amount of background due to nuclear reactions in the detector is 0.81% of the total counts in the main peak, while the total slit scattering contribution is 2.2%.

In order to present some of our experimental results we plot, as a function of the energy along the spectrum, the peak-to-valley ratio, defined as the ratio of the counts/channel at the maximum of the main peak to the counts/channel in the background. This ratio has to be referred to the experimental FWHM of the main peak, because the counts/channel in the main peak are, for a given number of particles transmitted, linearly dependent upon its FWHM, while the counts/channel in a smoothly varying background are not. While the peak-to-valley ratios thus obtained are certainly not of universal use we feel that they help in visualizing the limits to the measurable cross sections, i.e. those limits determined by the slit scattering effect in a typical counter experiment. The peak-to-valley ratios presented here are obtained from spectra like the ones above by subtracting the contributions due to reactions in the detector.

We summarize these results by considering separately the following regions of the spectrum: 1) the region within 200 keV of the main peak; 2) the region including the first 2 MeV of energy loss; 3) the remaining part of the spectrum corresponding to higher energy losses.

In region (1) we are unable to observe any appreciable slit-scattering. A typical example of the behavior in this region is shown in fig. 4. There, for 20 MeV protons, we present spectra obtained without slits (open counter) and with polished, straight-edged, brass slits. A gaussian with the same

FWHM is also plotted for reference. The fact that the two experimental plots coincide proves that the long tail in the spectrum (visible also in fig. 2) is not due to slit-scattered particles. These data suggest that the response of a Si(Li) counter to a monochromatic beam is not a gaussian. Further evidence for this non-gaussian response is presented in fig. 5, where spectra obtained for different counters, for the particles and energies listed, are plotted as a function of the ratio of the energy difference from the main peak to the experimental FWHM. These spectra exhibit a gaussian shape above the peak but deviate appreciably from a gaussian on the low energy side. The deviation could be due to several effects: 1) elastic collisions in which the recoiling silicon nuclei do not lose energy as efficiently as lighter particles[4]); 2) poor charge collection in the detector, due to trapping; 3) electronic pile-up, which was shown to be a small effect by observing a pulser spectrum above the main peak.

The peak-to-valley ratios obtained for the first few MeV below the main peak (region (2)) are shown in fig. 6, for 50 MeV α's (top) and 20 MeV protons (bottom). Curves for straight-edged slits of the various materials are shown, together with those corresponding to an open-counter (no slit) geometry. The results can be summarized as follows: a) In all cases the peak-to-valley ratios drop sharply in the proximity of the main peak. This merely reflects the response of the counter in region (1). b) Tantalum and brass slits show a similar behavior for both alpha particles and protons. c) For 50 MeV α's there is a difference of about one order of magnitude in the peak-to-valley ratios for polished and unpolished slits. The fact that this difference is much less pronounced for 20 MeV protons, can be

understood in terms of their greater penetrating power. It will be shown later (sect. 4) that the requirement on surface polishing can be stated in more quantitative terms. d) In region (2) the behavior of the peak-to-valley ratios as a function of energy is flat, within the statistical errors.

In fig. 7 the peak-to-valley ratios plotted refer to brass slits of different profiles. The curve corresponding to an open counter is shown for reference. Straight-edged and large radius-of-curvature slits behave similarly in this energy region. Tapered slits or slits with a small radius-of-curvature give a peak-to-valley ratio which is lower by a factor 2-3, approximately 1 MeV below the main peak.

The results for region (3) (energy losses greater than 2 MeV) are presented in fig. 8, for 20 MeV protons. The upper figure shows the behavior of straight-edged slits of different materials; the lower figure shows the results for different profiles of brass slits. The curve obtained with an open counter exhibits many valleys, which are due to nuclear reactions in the detector. In the neighborhood of these valleys the slit scattering with polished slits is of the same order of magnitude. For all slits the peak-to-valley ratio reaches a minimum at about 8-10 MeV (an energy loss close to 50%) where it is approximately a factor of two lower than at the high and low energy extremes of the spectrum. It is understandable that the large and small radius slits give worse results in the region of high energy loss since a part of their profile is transparent to the incident particles. However the shape of the distribution is very similar for the different profiles.

Some conclusions that are of general value can be drawn from the above results. These include: the importance of good surface polishing; the near

equivalence of brass and tantalum as slit material; the similar behavior of straight-edged slits and large-radius slits for low ($\approx$ 10% maximum) energy losses, and the superiority of the straight-edged slits in the remaining part of the spectrum. It is, however, difficult to predict the peak-to-valley ratios for other energies and particles. In addition these results are only valid for a nearly parallel beam, as employed in the present experiment. This is not the situation in a typical scattering experiment.

4. Comparison with Theory

It is instructive to compare some of our experimental data with a theory developed by Courant[2]) in 1951, which evaluates the slit scattering effect in a closed and simple form. We recall the expressions derived by Courant for a parallel beam, in order to compare the results directly with our measurements. The hypotheses underlying the calculations are: 1) a continuous energy loss in a slit and 2) a constant scattering cross section. Then for the case of: a) a parallel beam; b) straight-edged slits; and c) slits with a thickness equal to the stopping thickness, the following formula gives the effective slit width increase, d, for particles scattered to all angles with an energy loss between 0 and ΔE.

$$d = \frac{2}{(3\pi)^{1/2}} \cdot \frac{x^{3/2}}{W} \qquad (1)$$

Where x is the range in the slit material corresponding to an energy loss equal to ΔE and W is defined by:

$$W^2 = \frac{A}{Z^2 \pi N \rho} \cdot \left(\frac{E_{inc}}{(ze)^2}\right)^2 \cdot \left[\ln(181 \cdot Z^{-1/3})\right]^{-1} . \qquad (2)$$

In the usual notation A, Z and ρ refer to the slit material, while E_{inc} and ze refer to the incident particle energy and charge.

The term W, is physically related to the mean square of the angle of multiple scattering, $\langle \Theta \rangle^2_{av}$, in the slit material by:

$$\langle \Theta \rangle^2_{av} = \frac{4 \cdot x}{W^2} .$$

The Courant theory treats Θ^2 as a constant term with respect to the particle energy while in reality it has a $1/E^2$ dependence as the particle loses energy in the slit material. Refinements of the original Courant theory have been reported[3]). Their aim was to correct for the energy dependence of Θ^2 which, when neglected, underestimates d for large energy losses. The numerical calculations involved are, however, complicated and one misses the simple form of expression (1). Since the calculated corrections to the values of d amount to approximately 25% in most cases[2]), we feel that the additional accuracy is probably not that important. What is needed is a simple treatment which can be easily extended to a variety of experiments. For this reason only the Courant theory is compared with our data.

The comparison is presented in fig. 9, for brass, tantalum and aluminum straight-edged slits. For 20 MeV protons and 50 MeV alphas the percentage of particles scattered with energy losses between 0 and $\Delta E/E_{inc}$ is plotted as a function of $\Delta E/E_{inc}$. The size of the points is a measure of the

statistical errors. All points are calculated directly from the spectra, after subtracting the reaction contribution. The theoretical curves have been computed as the ratio of d, (formula (1)), to the slit width of 2 mm. The comparison, one should remember, is between absolute values, experimental and theoretical, with no normalization factors. The agreement is very good up to energy losses of about 50%. The theoretical curves are lower than the experimental values at higher energy losses: however, the difference is never more than 20%.

The importance, for this kind of comparison, of an almost perfect straight-edged profile can be seen in fig. 10. Here, for 20 MeV protons and 50 MeV α's incident on brass slits, we plot the percentage of particles scattered for the curved profiles, (i.e., the large-radius and small-radius slits described previously).

The theoretical energy spectrum of the slit-scattered particles, which is related to the experimental peak-to-valley ratios previously reported, is given by the differential, with respect to energy, of (1). Since the theoretical curve given by (1) has a zero derivative for an energy loss $\Delta E = 0$, the slit-scattering effect vanishes at the main peak and increases rapidly in the first few MeV reading a maximum of about 50% energy loss. This result is, however, only strictly valid for the present case of a parallel beam.

Finally, it is clear that one can use the values of d, calculated from (1), to get some insight into the problem of surface finishing. Depending upon the energy region of the spectrum in which one is interested, the degree of polishing should be such that the corresponding d/2 value be

larger than, or at least of the same order of magnitude as the surface irregularities. As an example, the values of d involved for the present set of experimental data are shown, in fig. 11. The degree of polishing must be very high if the region of interest includes the first 10% - 20% of the energy range.

5. Concluding Remarks

We believe that the present experiment has shown, in a sufficient variety of cases, that the Courant theory can be used with some confidence to predict the amount of the slit-scattering effect for a parallel beam. The theory also provides a mathematical technique to treat the non-parallel beam case. This extension seems justified since no other physically restrictive assumptions are needed and only the mathematical treatment becomes more involved.

Since it is the case of a non-parallel beam which is of direct interest in an actual scattering experiment, computations have been carried out in order to evaluate the relevant slit scattering effects. Preliminary calculations indicate that for a non-parallel beam, with a divergence of $\pm 0.4°$, the peak-to-valley ratios, in the region a few MeV below the main peak, can be as much as a factor of 3 to 4 lower than the values found in the present experiment.

These results and their implications with respect to slit design for non-parallel beams will be the subject of a forthcoming paper.

Acknowledgments

The authors wish to thank Dr. B. G. Harvey for his support and continuous interest in this work, the cyclotron crew and the mechanical shop staff, notably D. K. Fong and F. Hart for their skillful cooperation in the preparation of this experiment. One of us (A.D.B.) would like to acknowledge support in the form of a postdoctoral fellowship from the National Science Foundation.

References

[1]) D. A. Smith, Scattering of Protons from Collimators, Rutherford Laboratory Report N.I.R.L./R/60 (1963) 101 (unpublished).

[2]) E. D. Courant, Multiple Scattering Corrections for Collimating Slits, Rev. Sci. Inst. 22 (1951) 1003.

[3]) E. J. Burge and D. A. Smith, Theoretical Study of Slit Scattering, Rev. Sci. Inst. 33 (1962) 1371.

[4]) J. Lindhard, V. Nielsen, M. Scharff, and P. V. Thoursen, Inst. Fys. Medd. Dan. Vid. Selsk. 33, No. 10 (1963).

Figure Captions

Fig. 1. Schematic experimental conditions. At the bottom the slit profiles used are sketched. From the left: straight edge, large radius-of-curvature, small radius-of-curvature, tapered on both sides by 10°, tapered on one side by 1°.

Fig. 2. Spectra obtained with 20 MeV protons for the first 2 MeV below the main peak: without slits at the top, with polished brass slits at the bottom.

Fig. 3. Spectra obtained with 20 MeV protons over the entire 20 MeV range: without slits at the top, with polished brass slits at the bottom.

Fig. 4. Spectrum of the main peak, for 20 MeV protons, with a FWHM of 14.7 keV. Measured with an open counter and with a polished, straight-edged, brass slit.

Fig. 5. Spectra of the main peak measured with the particles and energies listed, plotted as function of the ratio of the energy to the experimental FWHM.

Fig. 6. Peak-to-valley ratios referred to the quoted FWHM, obtained with 50 MeV α's (top) and 20 MeV protons (bottom), for the various slits listed.

Fig. 7. Peak-to-valley ratios measured with 20 MeV protons, referred to a FWHM of 20 keV, for the various brass slit profiles listed.

Fig. 8. Peak-to-valley ratios for 20 MeV protons, referred to a FWHM of 20 keV, over the entire range of 20 MeV. Results for different materials are plotted at the top, and for different profiles of brass slits at the bottom.

Fig. 9. Comparison of the experimental data for straight-edged slits of tantalum, aluminum and brass (for 20 MeV protons and 50 MeV α's) with the predictions of the Courant theory.

Fig. 10. Experimental data from brass slits of the different profiles listed, for 20 MeV protons and 50 MeV α's, together with the predictions of the Courant theory for straight-edged slits.

Fig. 11. Effective increase in the slit width, d, calculated according to the Courant theory (formula 1), for the slit materials, particles and energies listed.

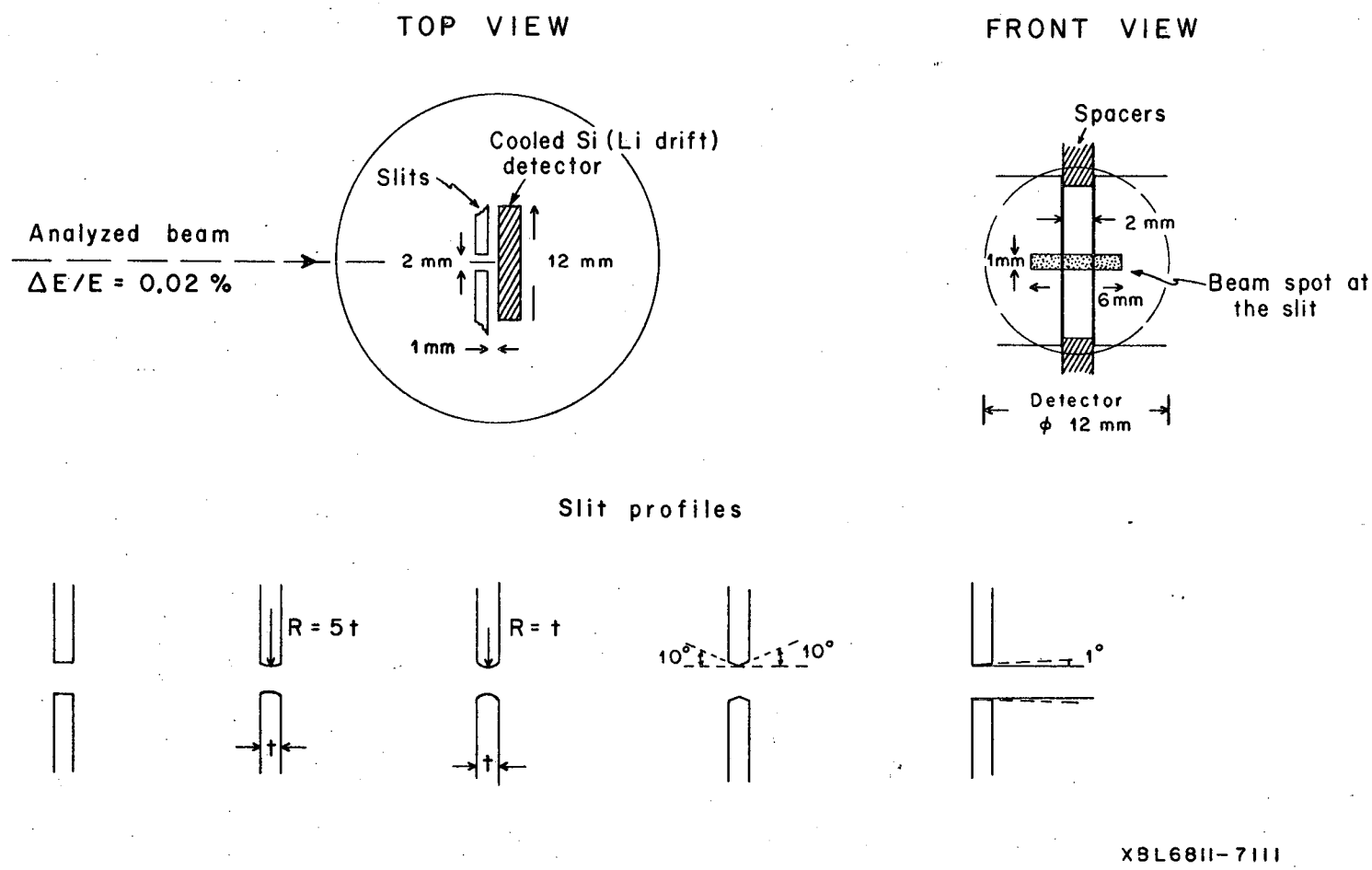
TOP VIEW
FRONT VIEW
Analyzed beam
ΔE/E = 0.02 %
Slits
Cooled Si (Li drift) detector
2 mm
12 mm
1 mm
Spacers
2 mm
1mm
6mm
Beam spot at the slit
Detector
ϕ 12 mm
Slit profiles
R = 5t
R = t
t
t
10°
10°
1°
XBL6811-7111

Fig. 1.

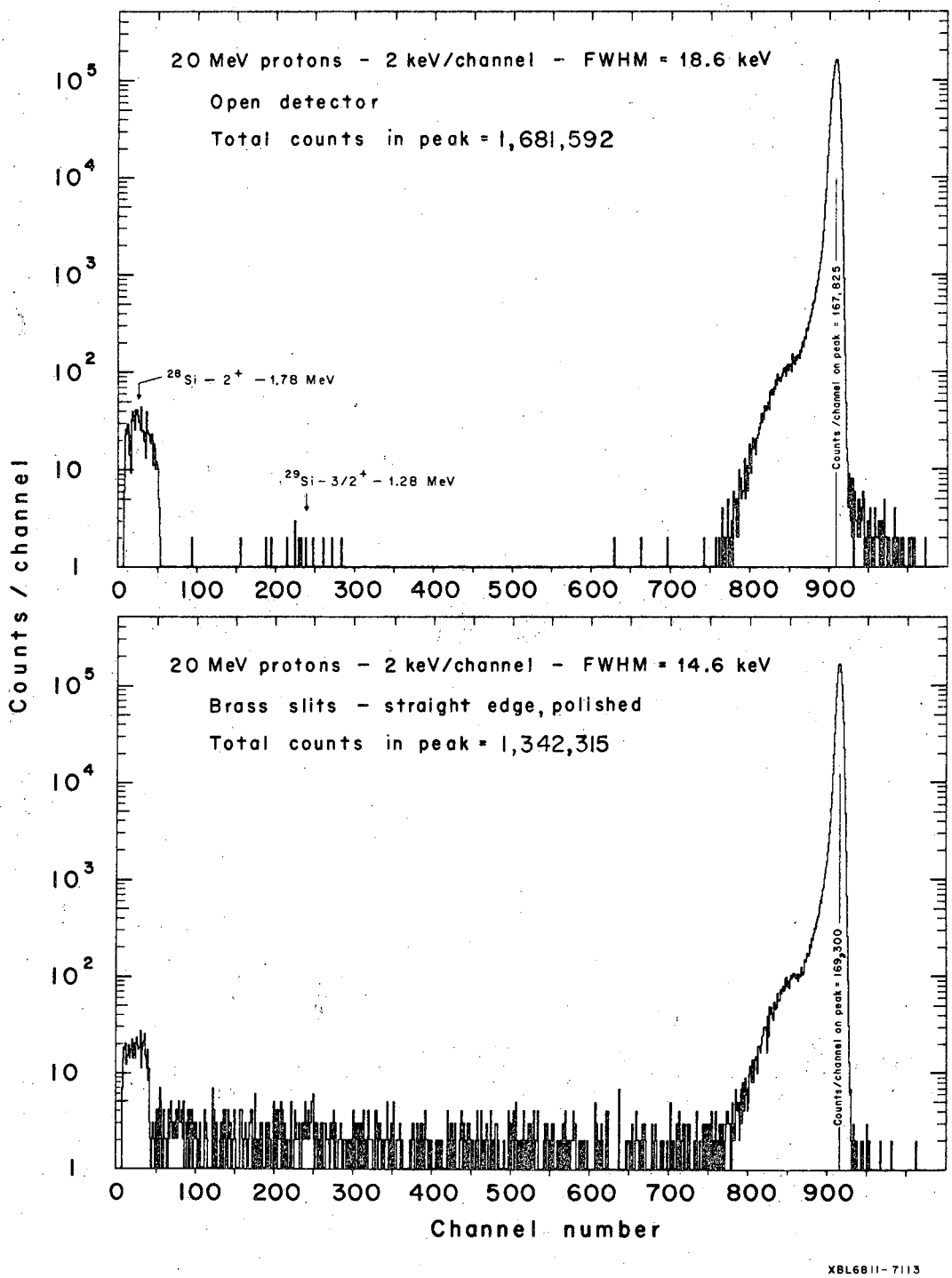
20 MeV protons - 2 keV/channel - FWHM = 18.6 keV
Open detector
Total counts in peak = 1,681,592
^{28}Si - 2$^+$ - 1.78 MeV
^{29}Si - 3/2$^+$ - 1.28 MeV
Counts/channel on peak = 167,825
20 MeV protons - 2 keV/channel - FWHM = 14.6 keV
Brass slits - straight edge, polished
Total counts in peak = 1,342,315
Counts/channel on peak = 169,300
Counts / channel
Channel number
XBL6811-7113

Fig. 2.

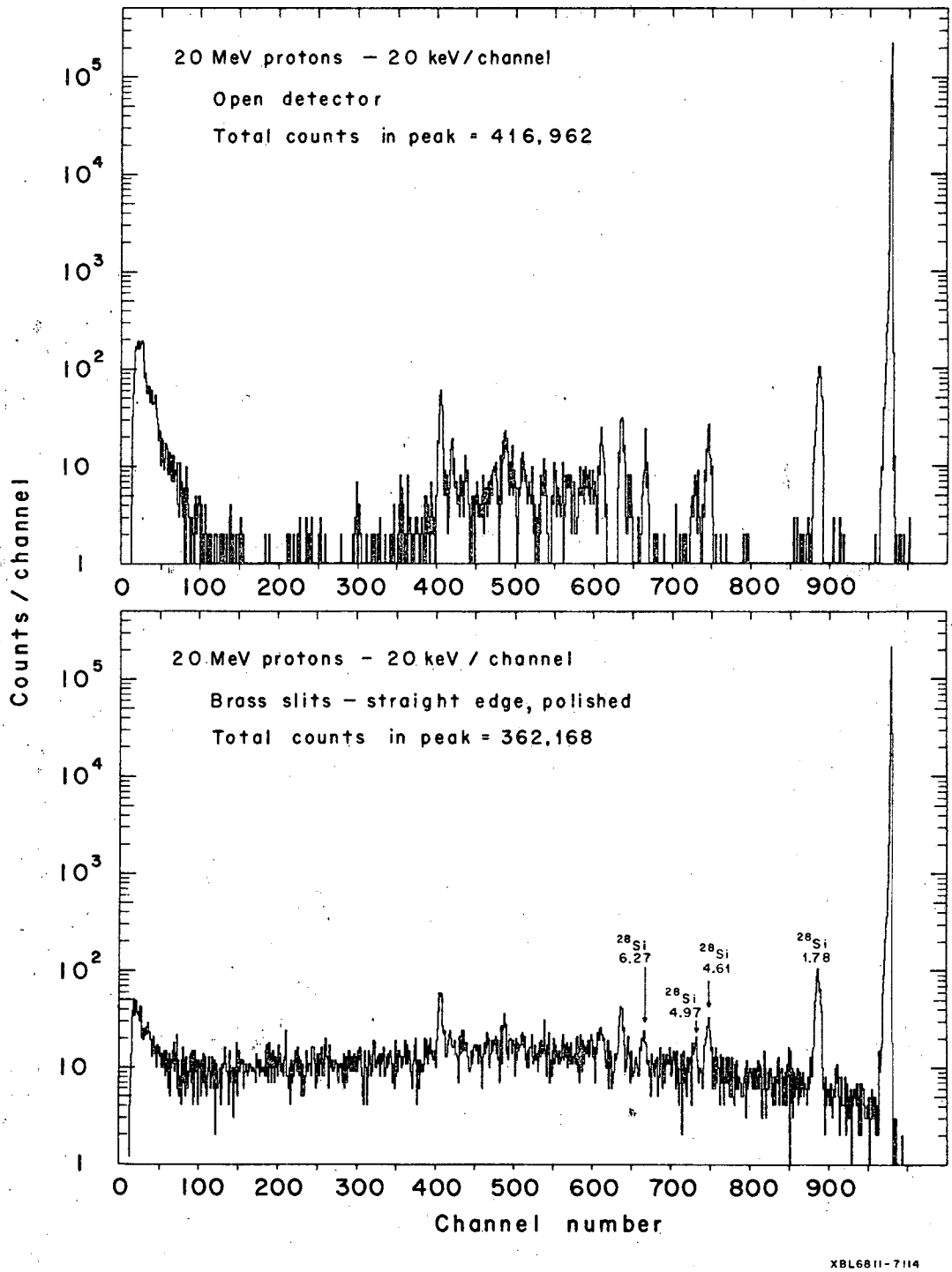
20 MeV protons — 20 keV/channel
Open detector
Total counts in peak = 416,962
20 MeV protons - 20 keV / channel
Brass slits — straight edge, polished
Total counts in peak = 362,168
^{28}Si 6.27
^{28}Si 4.97
^{28}Si 4.61
^{28}Si 1.78
Counts / channel
Channel number
XBL6811-7114

Fig. 3.

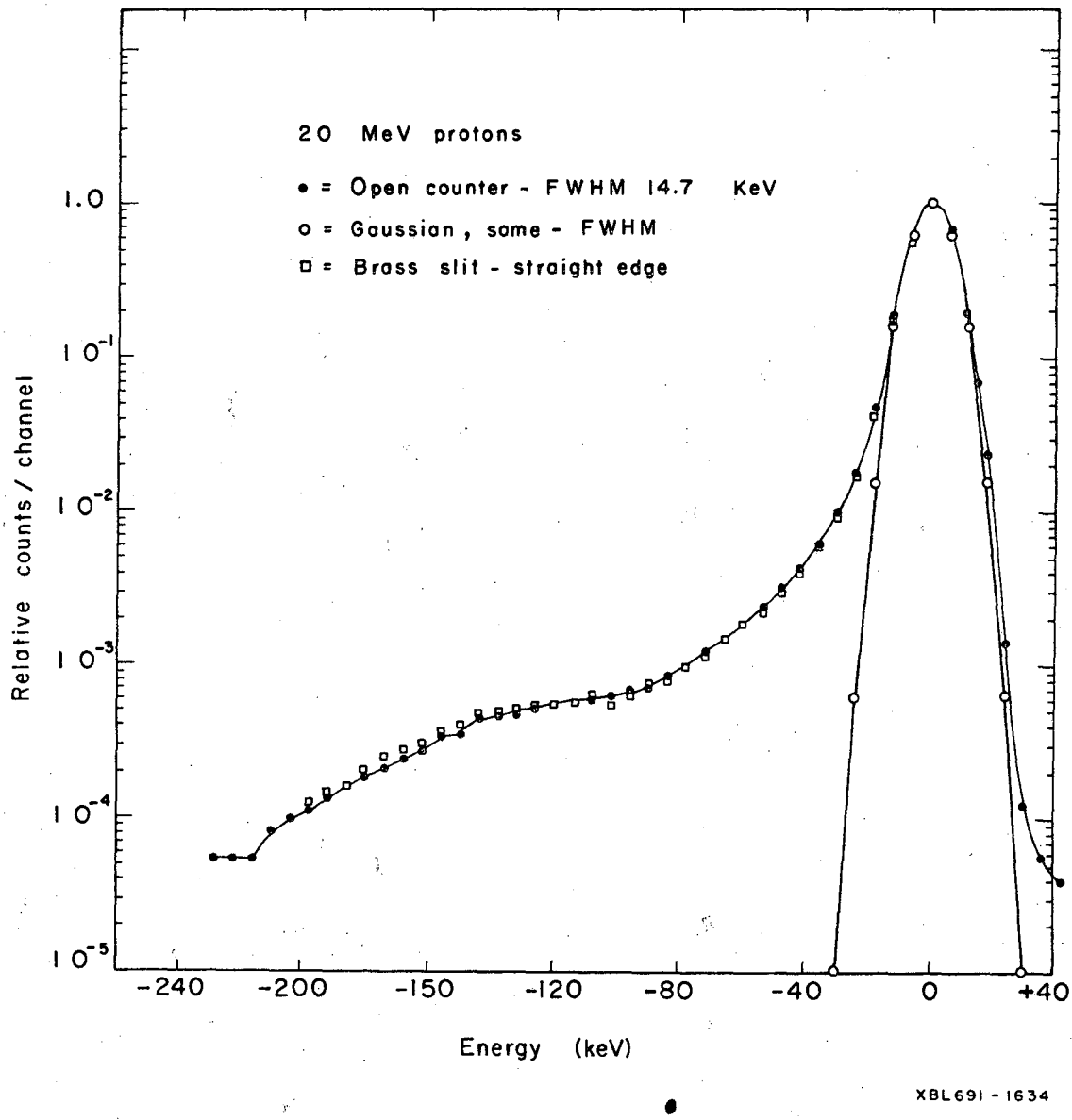
20 MeV protons
• = Open counter - FWHM 14.7 KeV
o = Gaussian, same - FWHM
□ = Brass slit - straight edge
1.0
10^-1
10^-2
10^-3
10^-4
10^-5
Relative counts / channel
-240
-200
-150
-120
-80
-40
0
+40
Energy (keV)
XBL691-1634

Fig. 4.

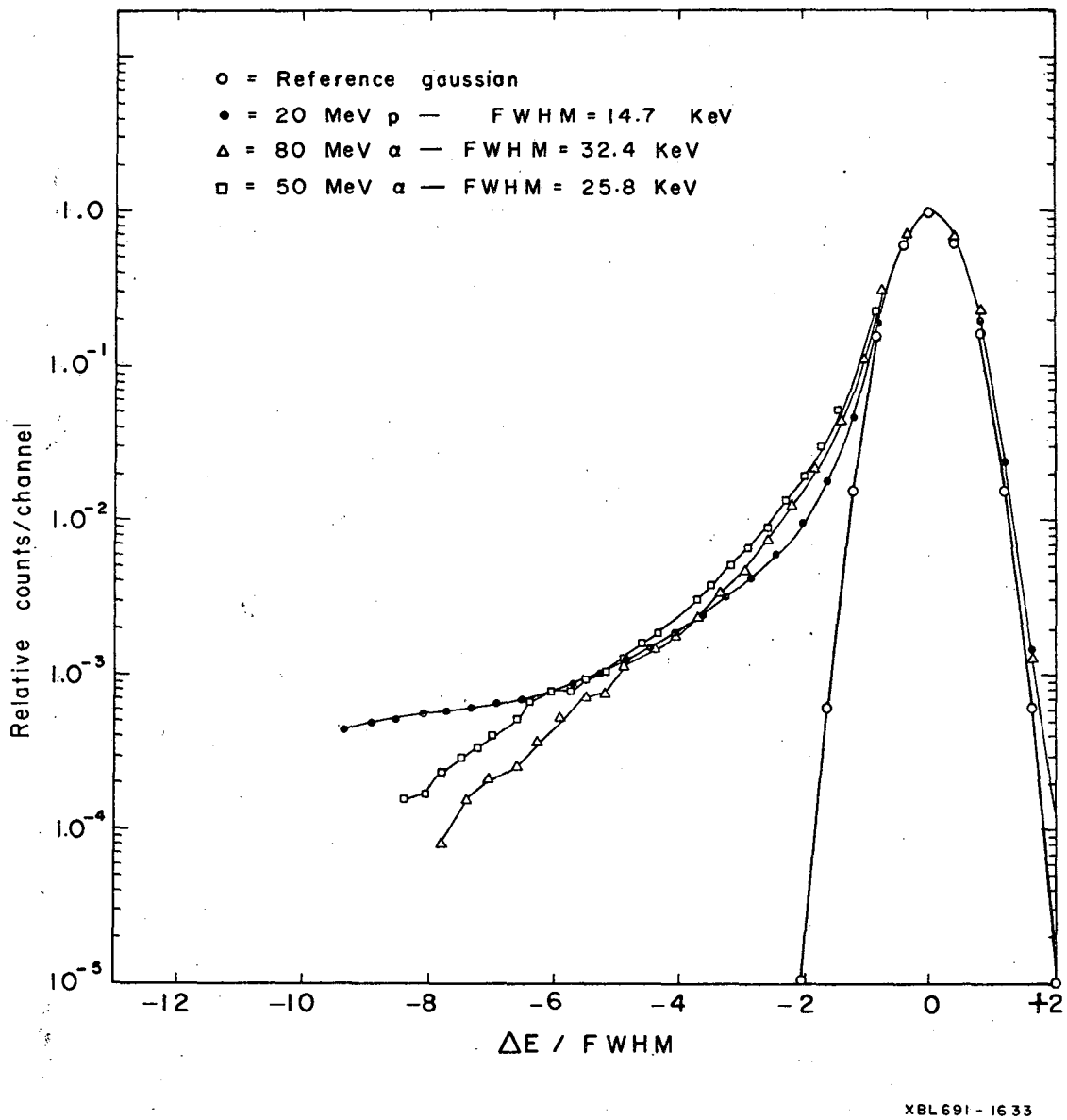
o = Reference gaussian
• = 20 MeV p — FWHM = 14.7 KeV
Δ = 80 MeV α — FWHM = 32.4 KeV
□ = 50 MeV α — FWHM = 25.8 KeV
1.0
1.0⁻¹
1.0⁻²
1.0⁻³
1.0⁻⁴
10⁻⁵
Relative counts/channel
-12
-10
-8
-6
-4
-2
0
+2
ΔE / FWHM
XBL691-1633

Fig. 5.

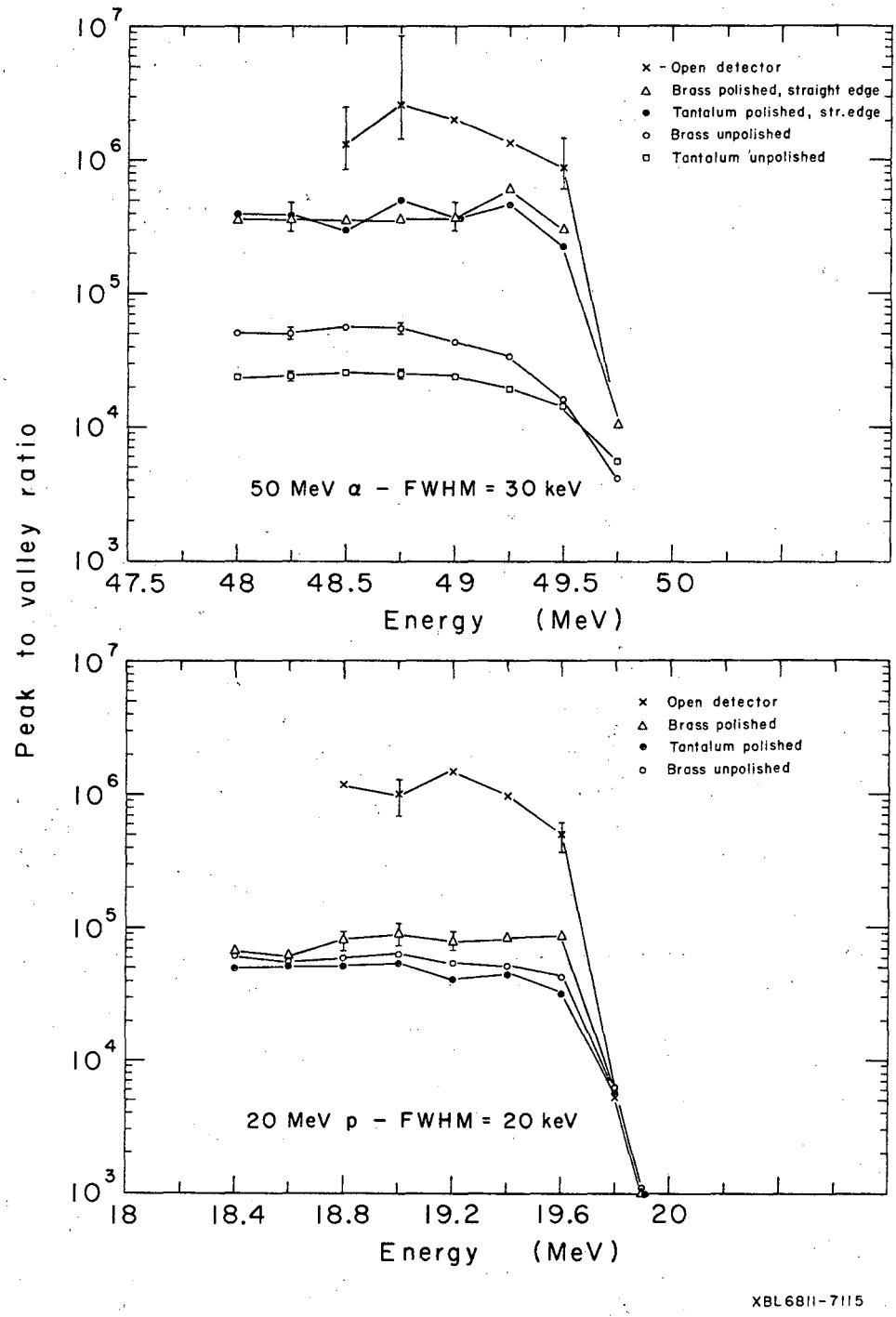
Peak to valley ratio
× - Open detector
△ Brass polished, straight edge
● Tantalum polished, str.edge
○ Brass unpolished
□ Tantalum unpolished
50 MeV α - FWHM = 30 keV
Energy (MeV)
× Open detector
△ Brass polished
● Tantalum polished
○ Brass unpolished
20 MeV p - FWHM = 20 keV
Energy (MeV)
XBL6811-7115

Fig. 6.

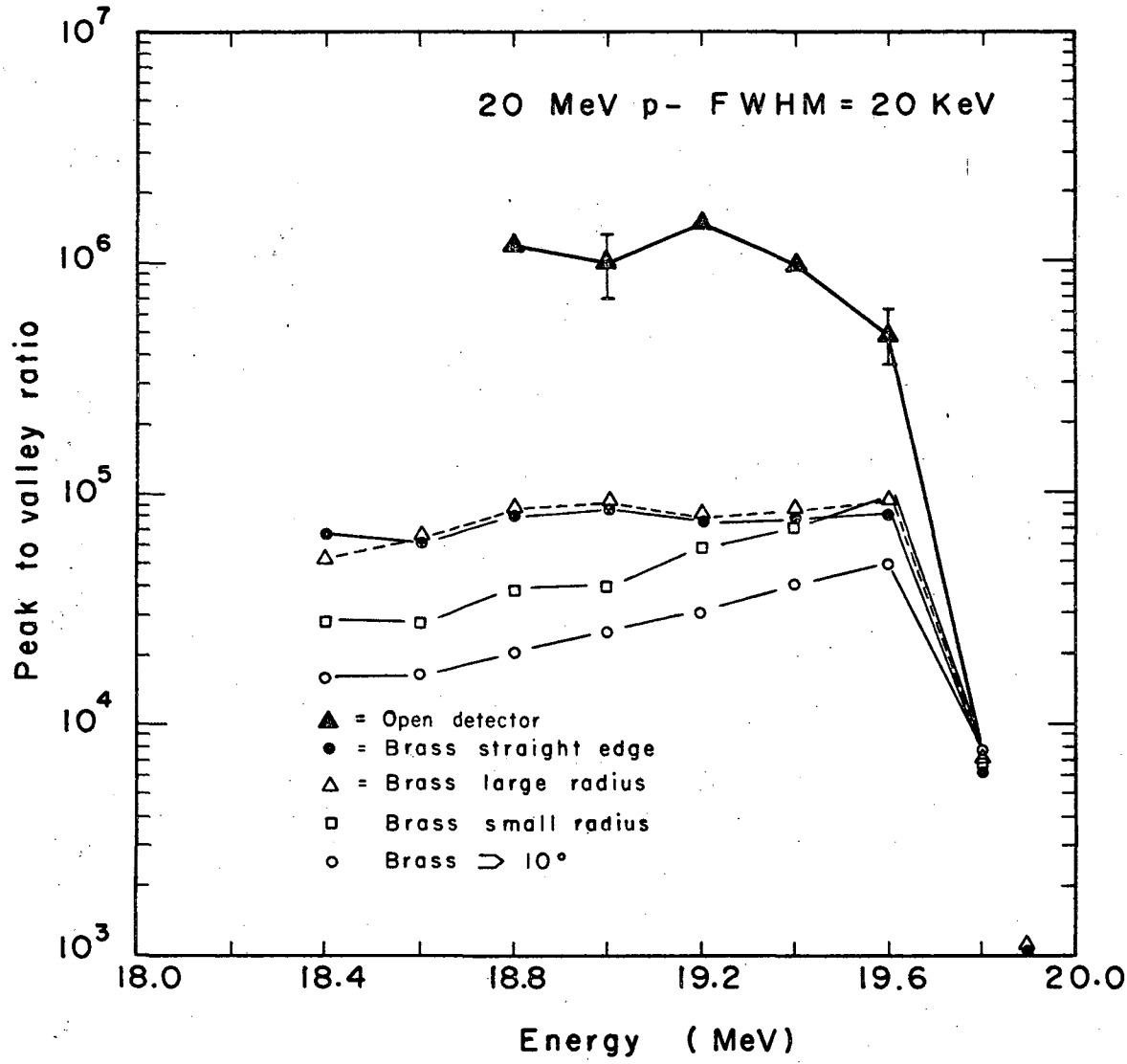

XBL691- 1632

Fig. 7.

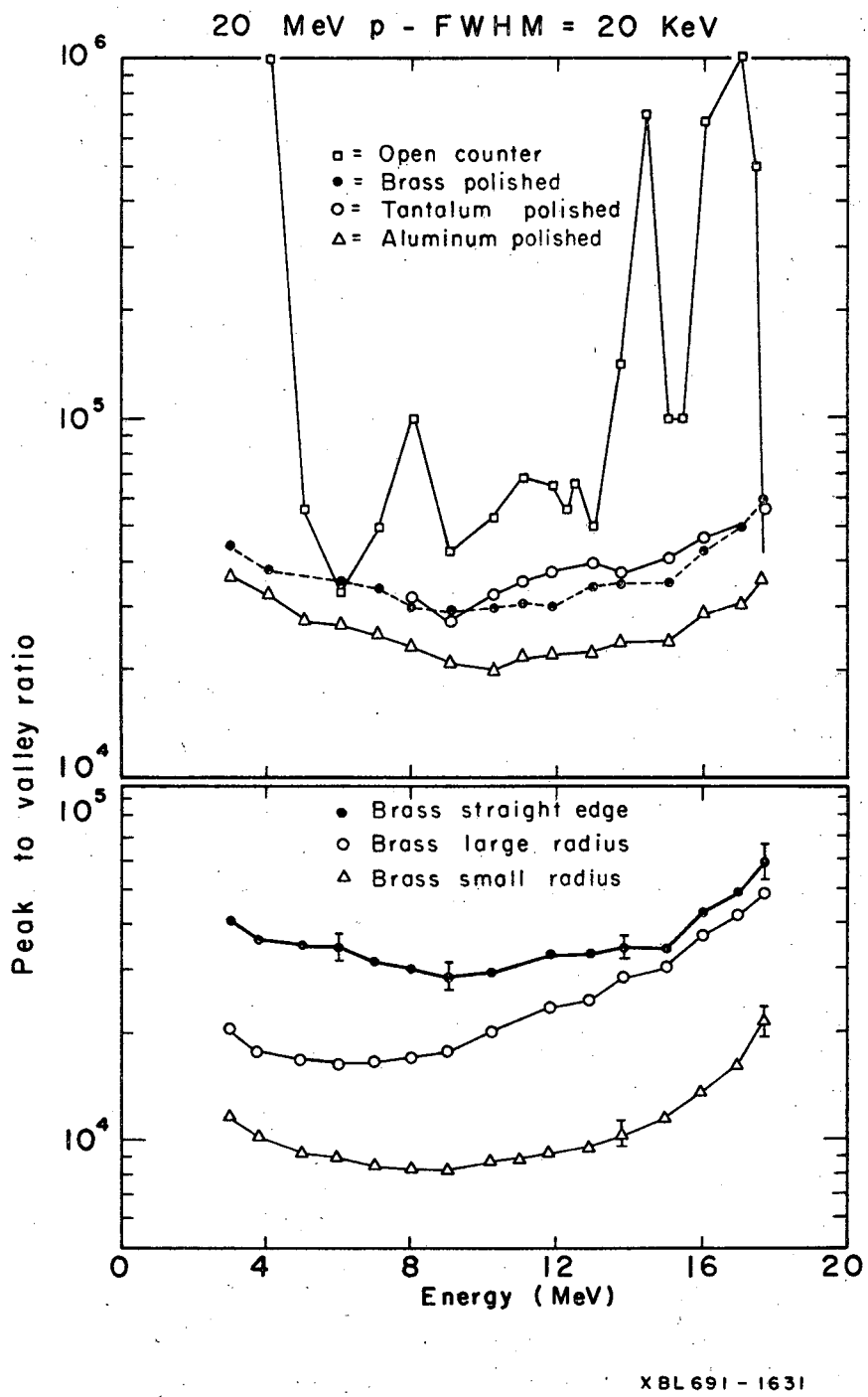
20 MeV p - FWHM = 20 KeV
□ = Open counter
● = Brass polished
○ = Tantalum polished
△ = Aluminum polished
● Brass straight edge
○ Brass large radius
△ Brass small radius
Peak to valley ratio
Energy (MeV)
XBL691-1631

Fig. 8.

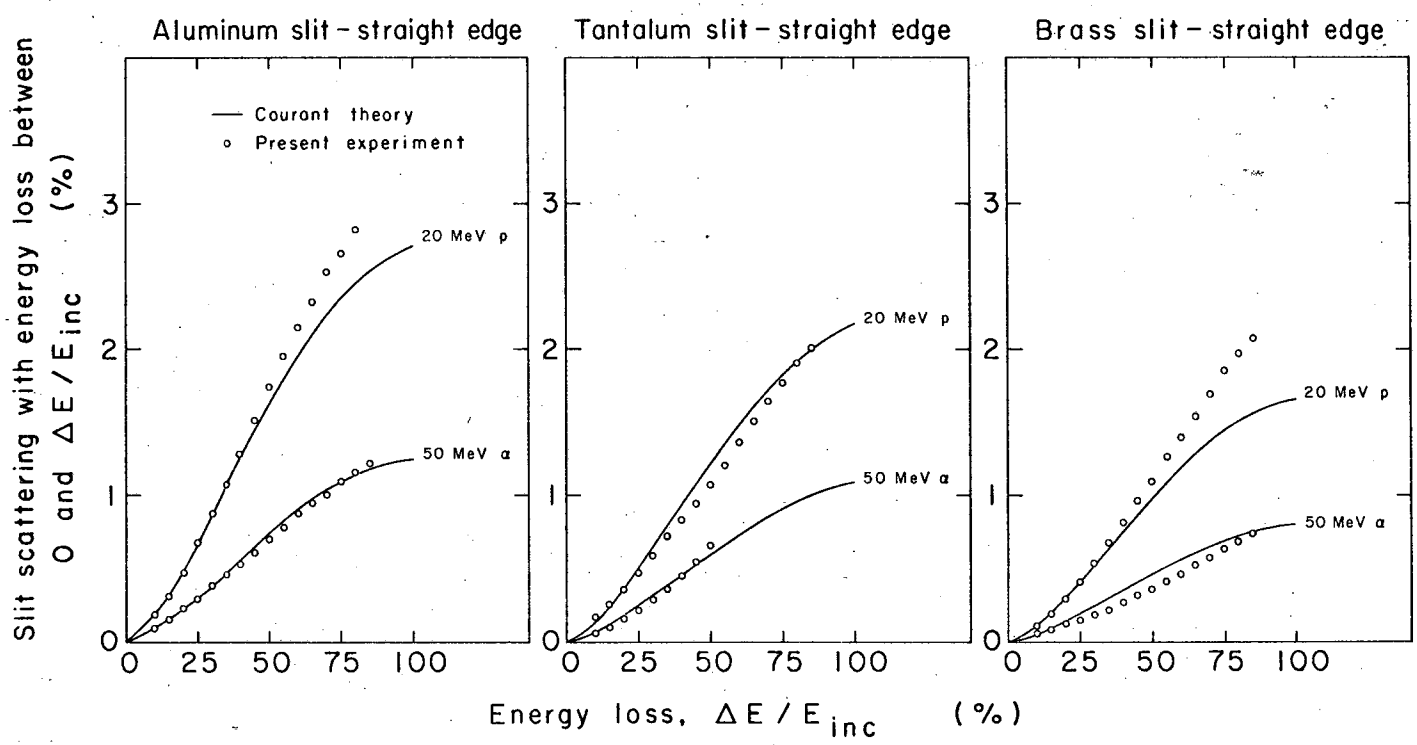
Aluminum slit - straight edge
Tantalum slit - straight edge
Brass slit - straight edge
Courant theory
Present experiment
20 MeV p
50 MeV α
Slit scattering with energy loss between 0 and ΔE / E inc (%)
Energy loss, ΔE / E inc (%)
0
1
2
3
0
25
50
75
100
XBL6811-7116

Fig. 9.

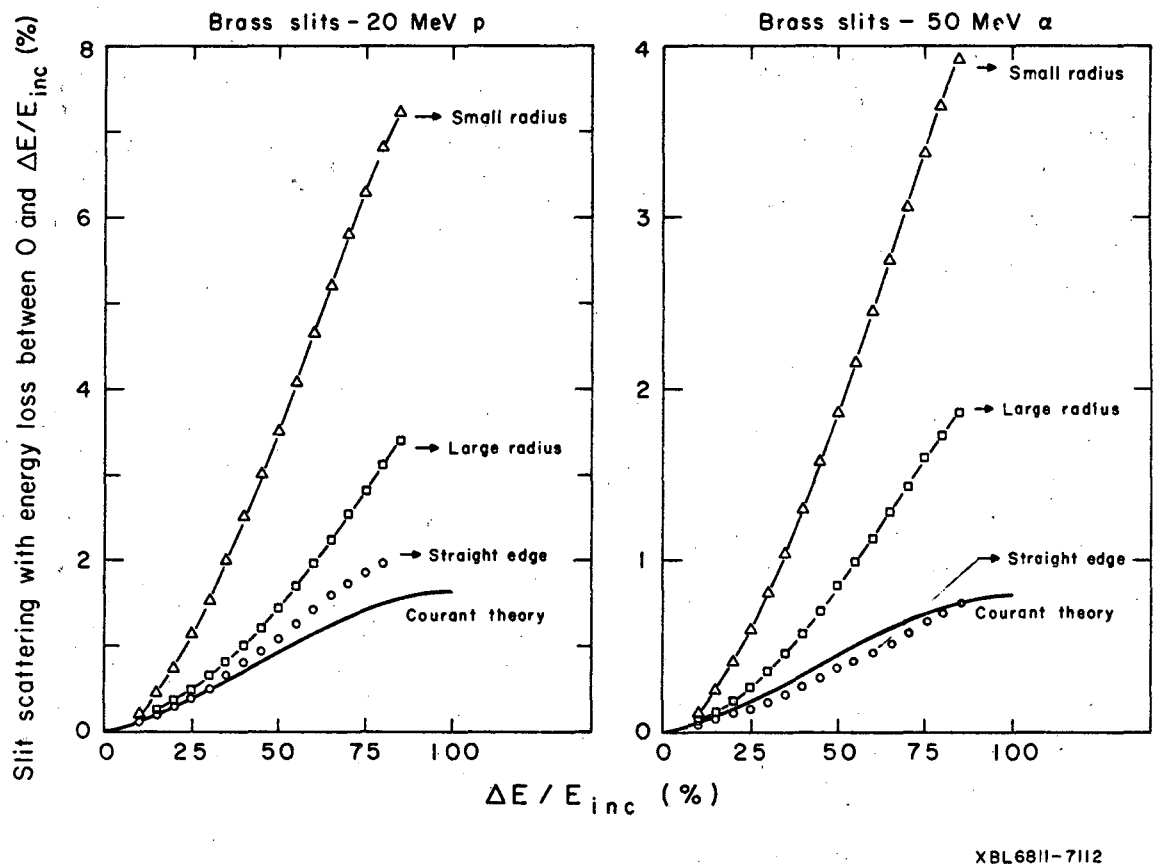
Brass slits - 20 MeV p
Brass slits - 50 MeV α
Small radius
Large radius
Straight edge
Courant theory
Slit scattering with energy loss between 0 and ΔE/E_inc (%)
ΔE / E_inc (%)
0
25
50
75
100
2
4
6
8
1
3
XBL6811-7112

Fig. 10.

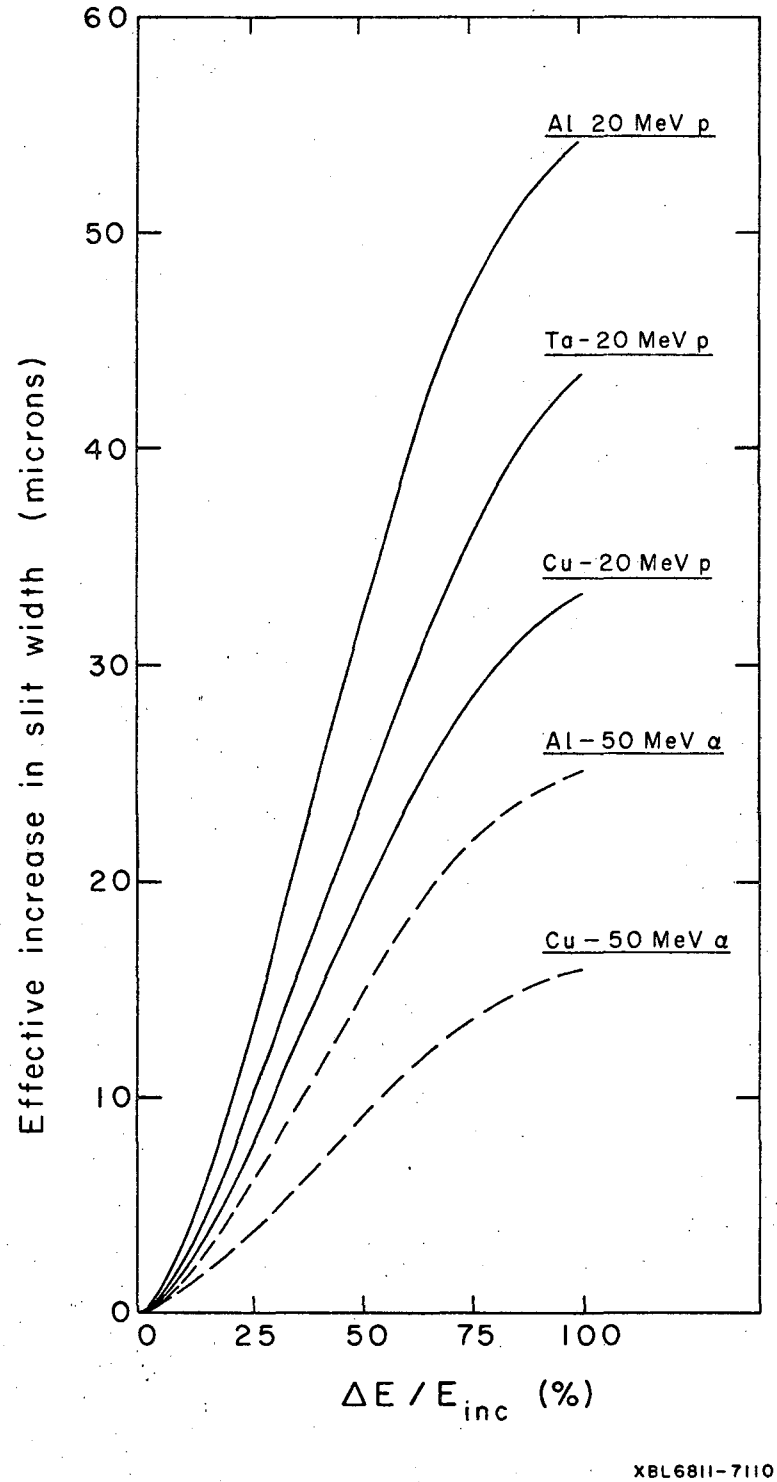
60
50
40
30
20
10
0
Effective increase in slit width (microns)
Al 20 MeV p
Ta-20 MeV p
Cu-20 MeV p
Al-50 MeV α
Cu-50 MeV α
0
25
50
75
100
ΔE / E_inc (%)
XBL6811-7110

Fig. 11.

LEGAL NOTICE

This report was prepared as an account of Government sponsored work. Neither the United States, nor the Commission, nor any person acting on behalf of the Commission:

A. Makes any warranty or representation, expressed or implied, with respect to the accuracy, completeness, or usefulness of the information contained in this report, or that the use of any information, apparatus, method, or process disclosed in this report may not infringe privately owned rights; or

B. Assumes any liabilities with respect to the use of, or for damages resulting from the use of any information, apparatus, method, or process disclosed in this report.

As used in the above, "person acting on behalf of the Commission" includes any employee or contractor of the Commission, or employee of such contractor, to the extent that such employee or contractor of the Commission, or employee of such contractor prepares, disseminates, or provides access to, any information pursuant to his employment or contract with the Commission, or his employment with such contractor.

TECHNICAL INFORMATION DIVISION
LAWRENCE RADIATION LABORATORY
UNIVERSITY OF CALIFORNIA
BERKELEY, CALIFORNIA 94720